RECOMMENDATIONS FOR CUBICLE SEPARATION IN LARGE-SCALE EXPLOSIVE ARENA TRIALS

T. Payne[1], A. Williams[1], T. Worfolk[1], S. Rigby[2]

[1] Home Office – Centre for Applied Science and Technology, Langhurst House, RH12 4WX.
[2] Department of Civil and Structural Engineering, University of Sheffield, Mappin Street, Sheffield S1 3JD.

ABSTRACT

In large-scale arena blast testing, a common and economical practice undertaken is to position several cubicle targets radially around a central charge. To gain maximal benefit from this, targets should be positioned at their minimum permissible separation at which no blast wave interference is sustained from neighbouring obstructions. This interference typically occurs either when targets positioned at the same stand-off range are too close creating an amplification effect where a superposition forms between the incident blast wave and the reflected wave off the cubicle, or, where a target is positioned in the region behind another target, which causes a shadowing effect with decreased magnitudes of pressure and impulse.

A comprehensive computational modelling study was undertaken using the hydrocode Air3D to examine the influence of cubicle positioning at different ranges on the surrounding blast wave pressure-time fields. A systematic series of simulations were conducted to show the differences in incident peak overpressure and positive phase impulse between free-field and obstructed-field simulation configurations. The predictions from the modelling study indicated that the presence of cubicle target obstructions resulted in differences in peak incident overpressure and positive phase impulse in nearby pressure waves. In all cases, at close separation distances, there were greater differences in peak pressure than positive phase impulse. However, with increased separation, peak pressure returned to free-field conditions sooner whilst differences in impulse remained significant, thus governing separation distance recommendations.

The simulations showed that, for targets at the same stand-off range, clear separations of between 3.88 m and 6.92 m were required to achieve free-field equivalency, depending on the distance from the charge to the target. For targets at different stand-off ranges an angle greater than 54.2° from the front corner of the cubicle has been shown to ensure free-field equivalent conditions. A bespoke recommendation table has been generated to provide precise positioning for cubicles at different stand-off ranges in a look-up matrix format that can be readily used by engineers in the field.

INTRODUCTION

When testing structural components under blast loading, a common practice in the UK and more widely is to test them in arena trials. In these trials, the structural components (e.g. walls, doors, glazing) are fitted into reaction structures and distributed around a central explosive charge. The aim of such tests is to isolate the effects of the target, consequently the test environment is kept intentionally simple to enable more predictable primary blast loading, minimising uncertainty and confounding variables.

The reaction structures, referred to herein as cubicles, are typically positioned at different stand-off ranges around the central charge. When a blast wave interacts with a cubicle, it reflects from it and diffracts around it, altering nearby pressure fields. Issues can arise in arena trials if the cubicles are positioned too close where interference effects from neighbouring cubicles and can change the nature of the loading. However, if cubicles are too dispersed, there is potential to more economically distribute targets. The mechanisms by which these interferences occur can be

broadly categorised as ‘shielding’ effects, where a reduced intensity is experienced behind the obstruction, or, an 'amplification' effect formed by a superposition of incident and reflected waves, magnifying the intensity of the resultant blast wave (Figure 1).

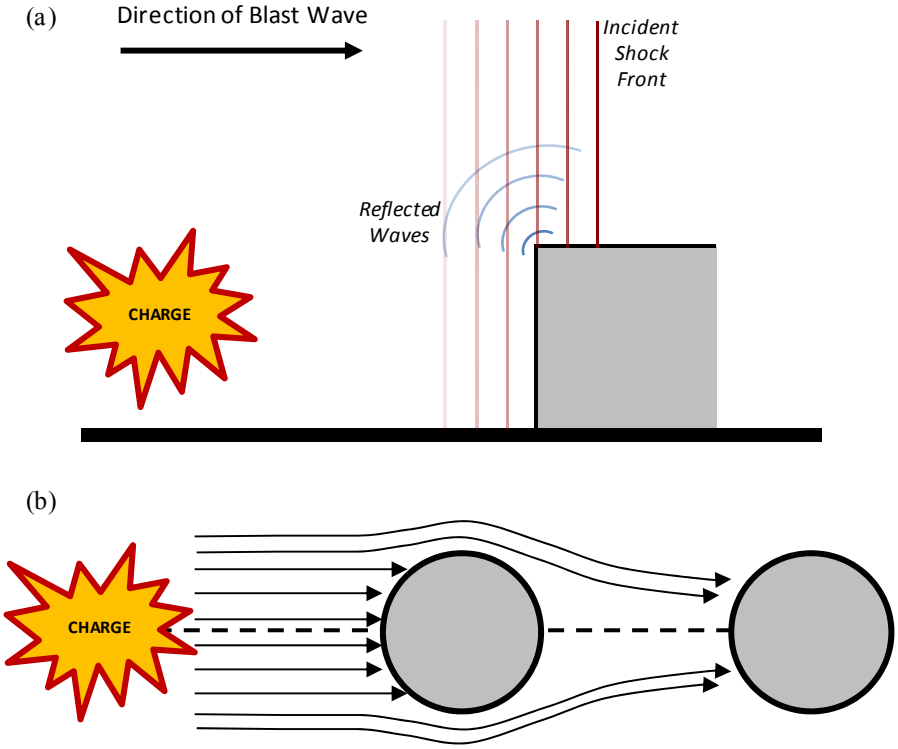

Figure 1: Schematics illustrating: (a) amplification and (b) shielding effects.

The local ‘clearing’ effects in blast-wave structure interactions from the loading of finite targets have been extensively studied (Rickman and Murrell, 2007; Shi *et al*., 2007; Ballantyne *et al.*, 2009; Rigby *et al*., 2014) and led to new perspectives on the mechanisms for estimating loading phenomena.

With consideration to the effects of these interactions more globally on nearby pressure fields, the most noteworthy studies in this area of relevance to this work were investigations into blast walls (Rose *et al*., 1995; Remennikov & Rose, 2007). The studies investigated the reductions in pressure and impulse in the immediate proximity behind the barrier providing an indication of the worth of the walls in different scenarios and practical design considerations. The study, however, was only concerned with walls of limited depth and as such did not consider the lateral effects associated with these blast wave interactions. More recent research in this area has focussed largely on blast wave effects in urban streetscape environments investigating multiple reflections and channelling effects. However, no study has specifically investigated the effects of cubicle positioning on neighbouring cubicles in arena test environments.

This study investigates the extent of interference effects presented by fixed target obstructions and provides a set of practical recommendations for use by engineers at test sites. The study primarily investigates cubicle stand-off ranges between 15 m and 50 m for 100 kg TNT

equivalent (TNTe) charge masses. These are typical parameters for blast trials conducted in the UK by the Centre for the Protection of National Infrastructure (CPNI).

METHODS

General Approach

Numerical modelling to investigate the differences in incident peak pressure (Ps+) and incident positive phase impulse (Is+) with a fixed target obstruction present. Data from these simulations was used to inform the degree of blast wave interference in the environment surrounding the cubicle.

Numerical Modelling

Hydrocode Air3D (Cranfield University, UK) was used throughout all simulations due to its verified accuracy over the relevant scaled ranges and its good representation of blast phenomenology relative to computational costs.

The numerical modelling test configuration (Figure 2) adopted is listed below:

- Simulations were each modelled in quarter symmetry with reflective boundaries closest to the planes of symmetry and transmissive boundaries at the extremes of the domain.
- A fixed target obstruction of dimensions: 3.5 m (W) × 3.95 m (H) and 3 m (D), representative of a wall testing cubicle structure, was modelled.
    - The fixed target was positioned at 5 m intervals from 15 – 50 m.
- Pressure gauges distributed in radial arcs at given stand-off distances from the plane of symmetry in the *y* axis.
    - 400 gauges were positioned evenly distributed at each stand-off distance.
    - Gauges were positioned at a height of 2 m (approx. ½ cubicle height).
    - Measurement locations were positioned in 5 m intervals between 15 – 50 m.

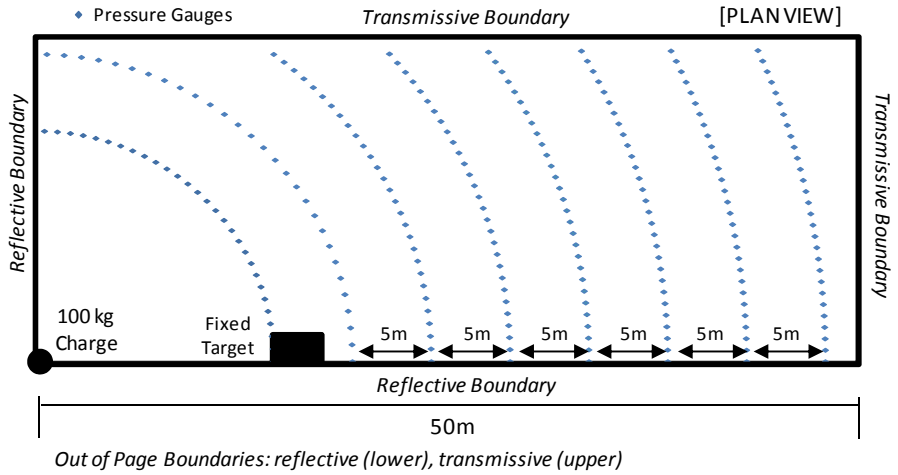

Figure 2: Schematic of simulation test configuration.

A mesh convergence study was conducted to identify the worth of incrementally finer computational meshes. Air3D predictions were compared to CONWEP (US Army Corps of Engineers, Engineer Research and Development Center, USA) hemispherical burst predictions for equivalent conditions to provide an indication of absolute accuracy of the model configuration. A study informed the use of 1 mm, 20 mm and 100 mm cell sizes for 1D, 2D and 3D simulations respectively.

A further validation was conducted prior to the main simulations investigating the diffraction effects exhibited by Air3D compared to experimental test results. Test data of reflected pressure-time histories on finite targets provided by the University of Sheffield (Tyas *et al*., 2011) were used to examine these effects. Figure 3 shows a comparison between Air3D simulation outputs and experimental data over relevant scaled distances. The study showed maximum differences in reflected positive phase impulse (Ir^+) of -2.86% from the experimental mean at these stand-off ranges.

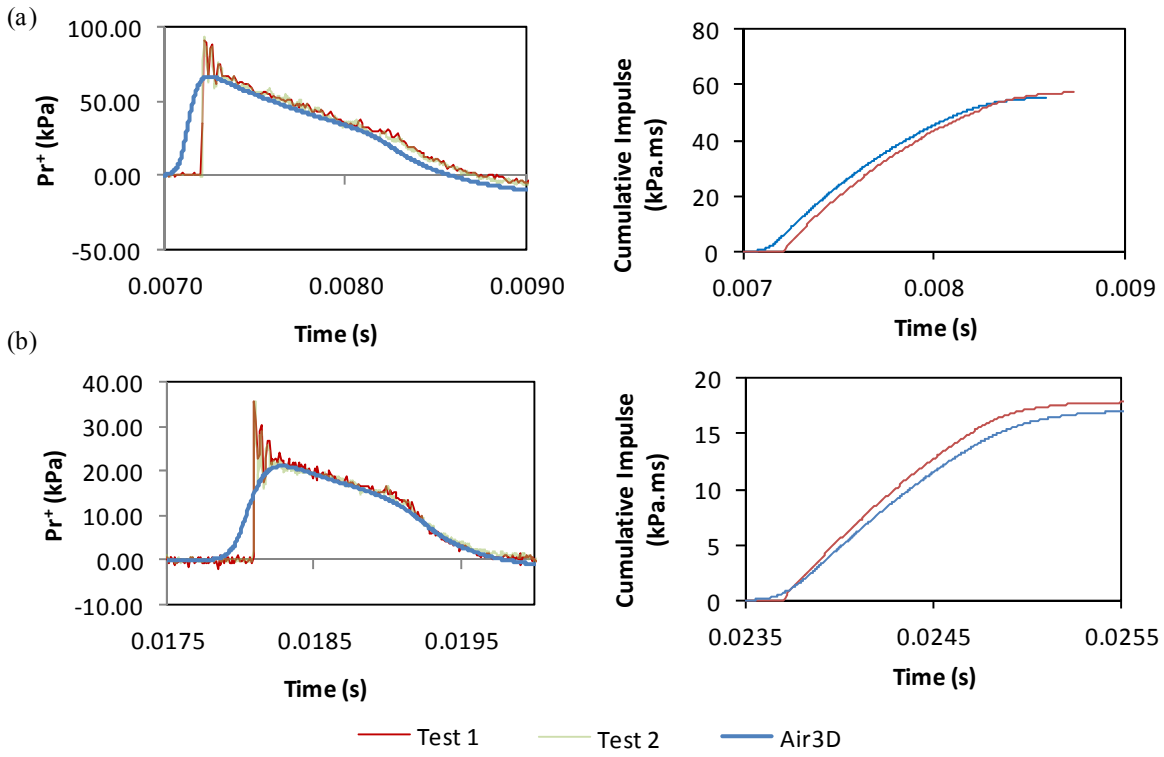

Figure 3: Comparison between experimental test data (Tyas *et al*., 2011) and Air3D predictions at: (a) 4 m and (b) 10 m stand-off ranges.

Post-processing

Incident pressure-time history outputs from the simulations were post-processed in MATLAB due to its robustness and capabilities handling large datasets. The post-processing procedure adopted has been listed below:

1. Ps^+ and Is^+ values identified at each gauge.

2. Percentage differences calculated between paired obstructed-field and free-field gauge outputs.

3. Identification of the co-ordinate location at which different percentage difference thresholds were exceeded.

4. Repetition for different fixed target ranges and measurement locations.

Given the co-ordinate positions at which thresholds were exceeded, separation distances were derived based on target location. For instances where:

- *Fixed target and measurement location at the same stand-off range:* separation calculated using the straight line distance from the corner of the target to the threshold point.

- *Fixed target and measurement location at different stand-off ranges*: separation determined by calculating the point of intersection between the threshold point and the charge origin, then, given by the straight line distance from the corner of the target to this intersection point (Figure 4).

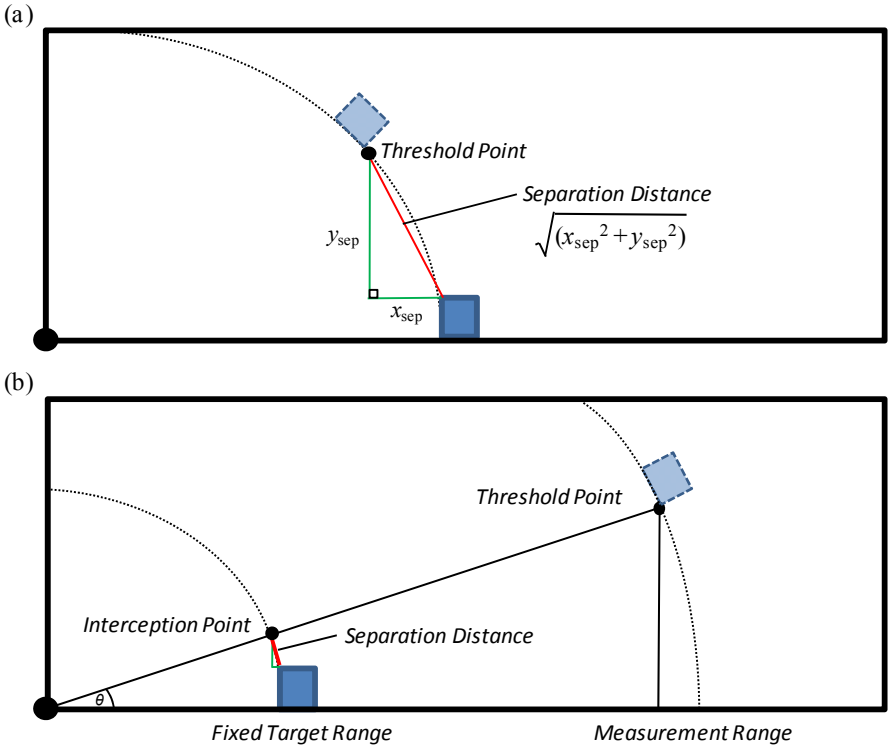

Figure 4: Schematic showing the calculations performed to determine minimum separation distances at different interference thresholds when the fixed target and measurement positions are at: (a) the same stand-off range; and (b) different stand-off ranges.

RESULTS

General trends

When the fixed target and measurement locations were at the same stand-off range, Figure 5 shows a representative example of the Ps^+ and Is^+ values recorded at different locations on the arc of pressure gauges. The graphs indicate that there is an amplification effect occurring whereby there is an increase in magnitudes of Ps^+ and Is^+ in the immediate proximity to the target. The graphs also show that Ps^+ values return to free-field equivalents at closer separation than Is^+ values.

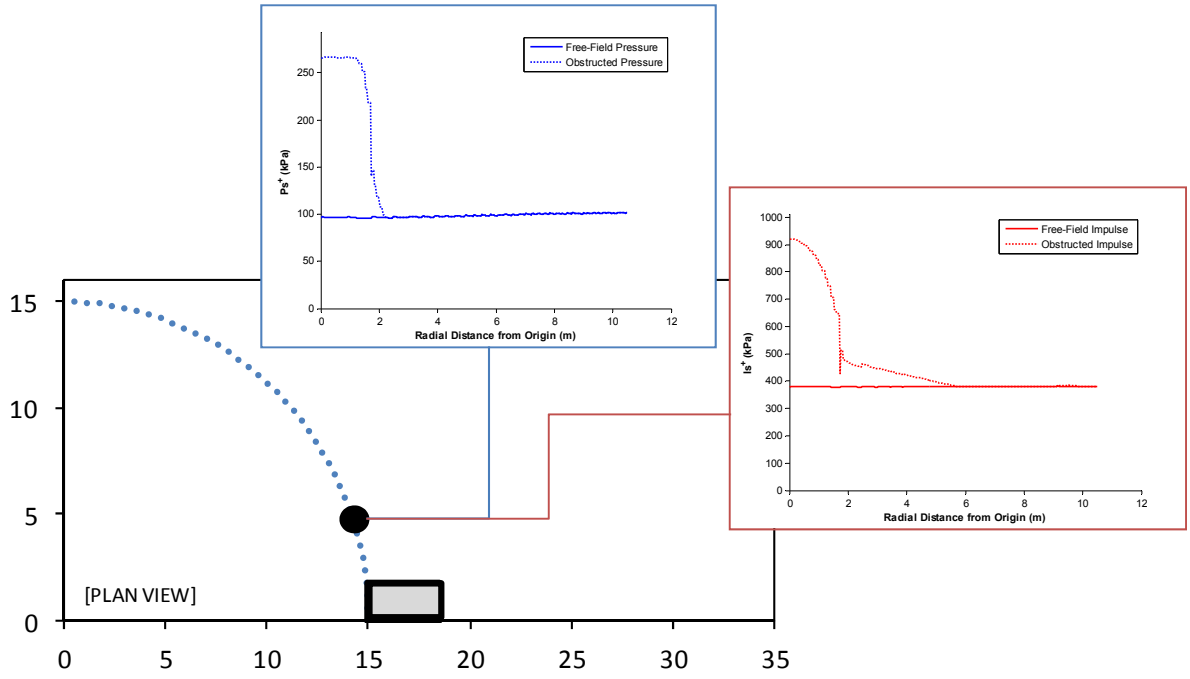

Figure 5: Graphs showing the differences in free-field and obstructed-field Ps^+ and Is^+ values for fixed target and measurement location at the same 15 m stand-off range.

Figure 6 shows a representative example of the data recorded when the fixed target and measurement range were located at different stand-off ranges. In this case, the obstructed-field Ps^+ and Is^+ values were significantly lower than free-field equivalents in the region behind the target. Similar to the same range simulations, Ps^+ values return to free-field magnitudes at closer separation than Is^+ values.

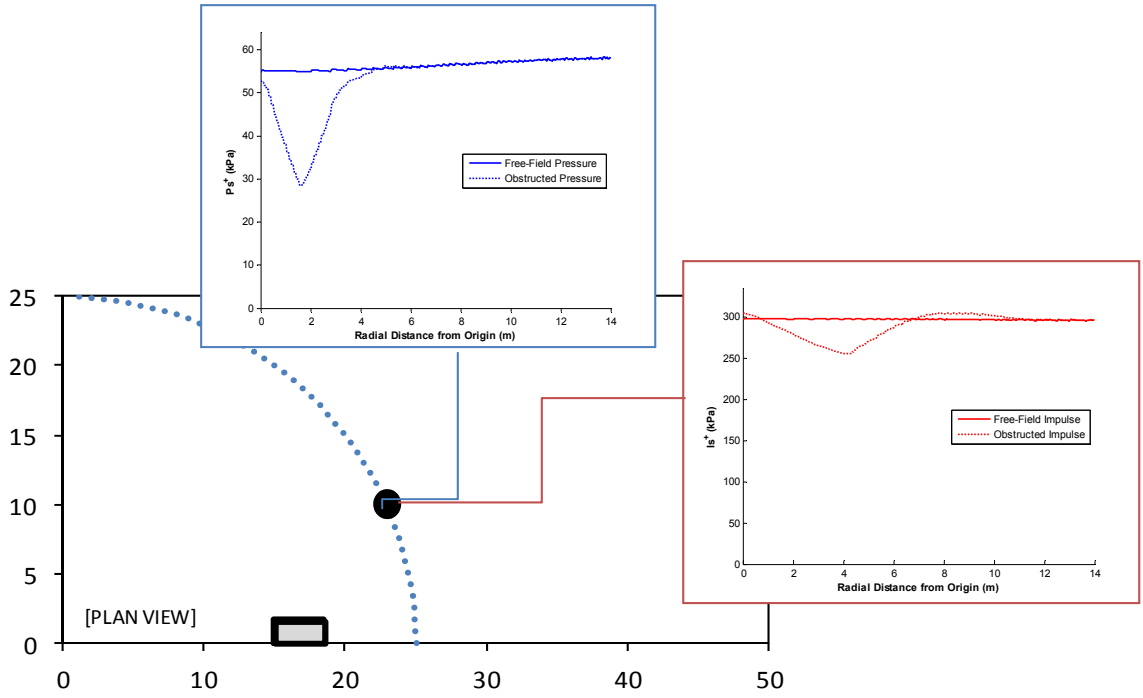

Figure 6: Graphs showing the differences in free-field and obstructed-field Ps^+ and Is^+ values for fixed target and measurement location at the different stand-off ranges.

Visualisations

Figure 7 shows a contour plot visualisation of the Ps^+ and Is^+ fields around a 15 m fixed target obstruction.

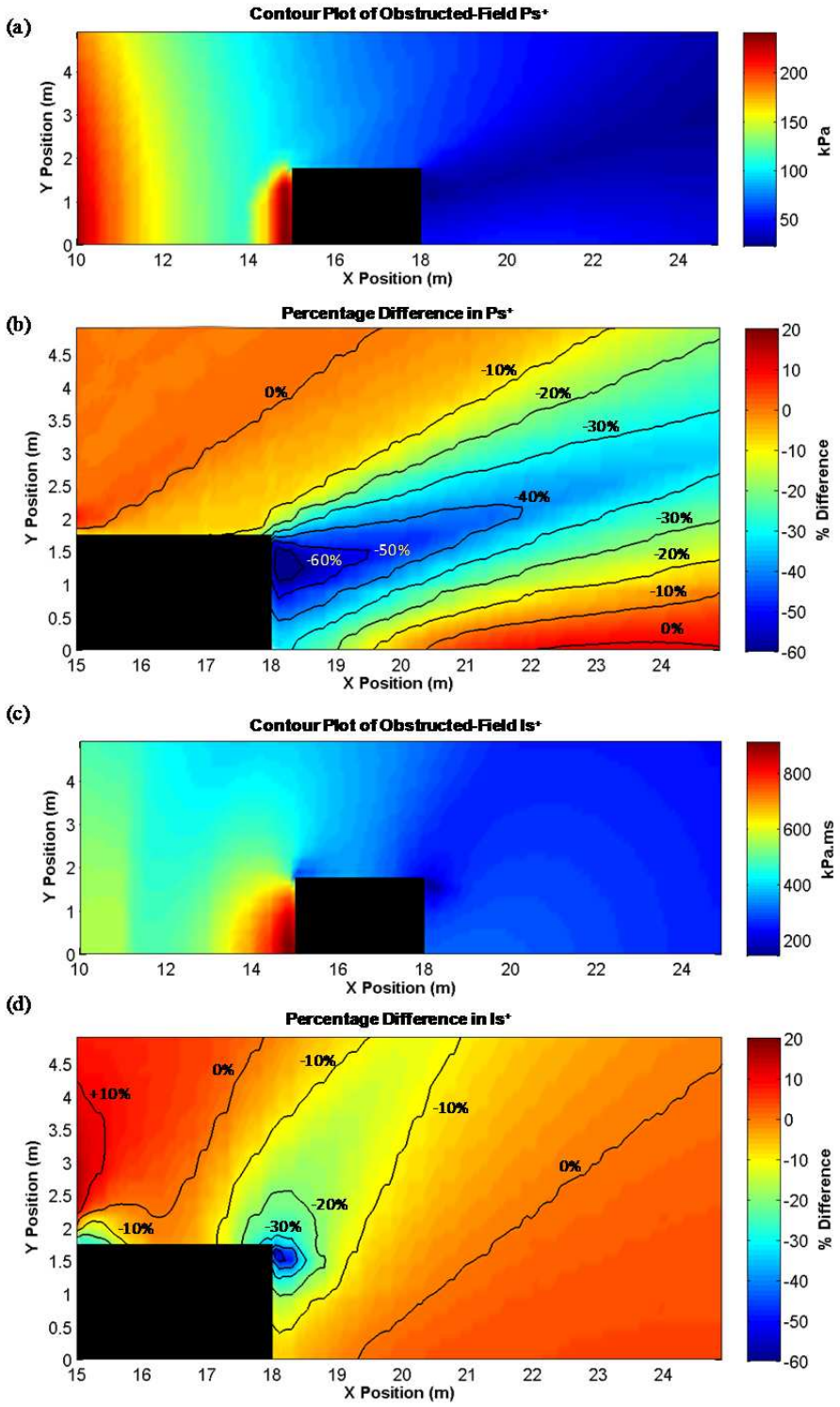

Figure 7: Visualisation showing contour plots round a fixed 15 m obstruction: (a) obstructed-field Ps+; (b) percentage differences in Ps+; (c) obstructed-field Is+; (d) percentage differences in Is+.

Assuming a linear angle from the front corner of the cubicle, Table 1 shows the angles for the limit of interference (free-field equivalence) for targets located at different stand-off ranges.

Table 1: Angle of the limit of interference from the front corner of target located at different stand-off ranges.

		Angle (°)	
		Ps^+	**Is^+**
Target Stand-off Range	15 m	36.4	54.2
	20 m	31.1	50.6
	25 m	28.0	49.3
	30 m	25.7	48.8
	35 m	24.3	49.5
	40 m	23.2	51.1

Recommendations

A recommendation table has been generated to inform cubicle target positioning in arena blast trials. Using the calculation method in Figure 4, Table 2 details the predicted separations necessary to achieve 0% interference for fixed target obstructions and variable targets between 15 m and 50 m.

Table 2: Recommended clear separation distances to achieve representative (0% interference) free-field Ps^+ and Is^+ values for fixed and variable targets at different stand-off ranges.

Fixed Target Location \ Variable Target Location	15 m	20 m	25 m	30 m	35 m	40 m	45 m	50 m
15 m	3.88	3.30	5.55	6.88	7.96	8.70	9.21	9.64
20 m		4.58	4.03	6.49	8.08	9.50	10.1	10.7
25 m			5.03	4.51	7.18	8.97	10.5	10.9
30 m				5.26	4.72	7.87	9.87	11.2
35 m					5.58	5.42	8.32	10.3
40 m						5.99	5.48	12.1
45 m							6.87	5.83
50 m								6.92

Effect of cubicle stand-off distance

The percentage differences in Ps+ for a 15 m fixed target obstruction have been compared to equivalent visualisations for fixed targets at 30 m and 45 m (Figure 8). It is evident that, when the fixed target is positioned at greater stand-off distances the peak percentage differences decrease. The angle for 10%, 20% and 30% difference thresholds remains relatively constant throughout, however, the 0% threshold begins at the front corner of the cubicle at 15 m but the rear of the cubicle at 30 m and 45 m; the 0% angle also appears more acute at 30 m and 45 m, which is consistent with the results in Table 1.

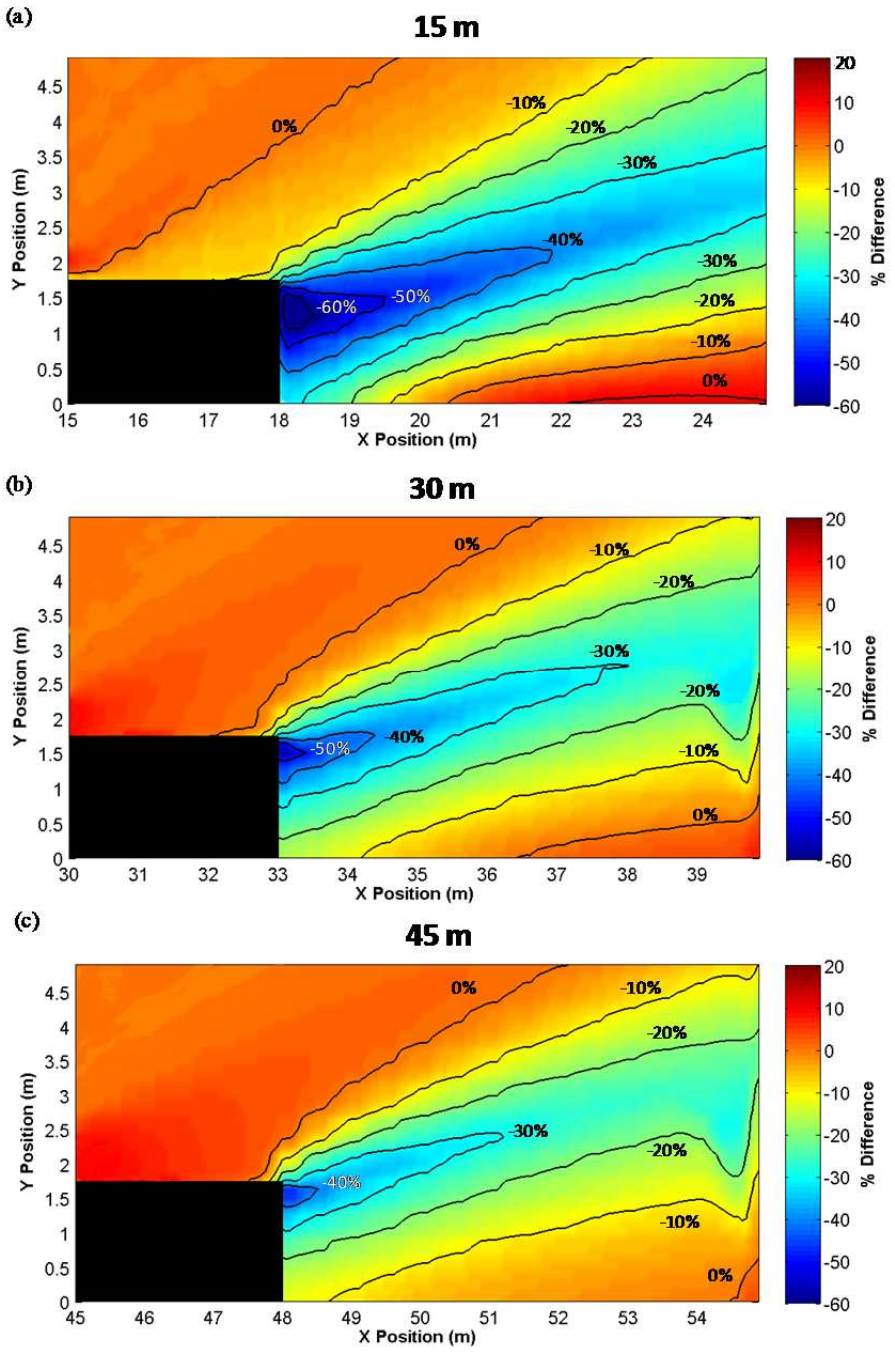

Figure 8: Visualisations showing percentage differences in Ps^{+} around fixed target obstructions at: (a) 15 m; (b) 30 m and (c) 45 m.

Similarly, Figure 9 compares differences in Is^+ fields around fixed targets at 15 m, 30 m and 45 m stand-off ranges. The magnitudes of peak percentage differences attained decrease at greater stand-off ranges. The angles for the limit of interference (0%), however, remained relatively constant at 15 m, 30 m and 45 m fixed target stand-off ranges in each case stemming from approximately 1 m target depth.

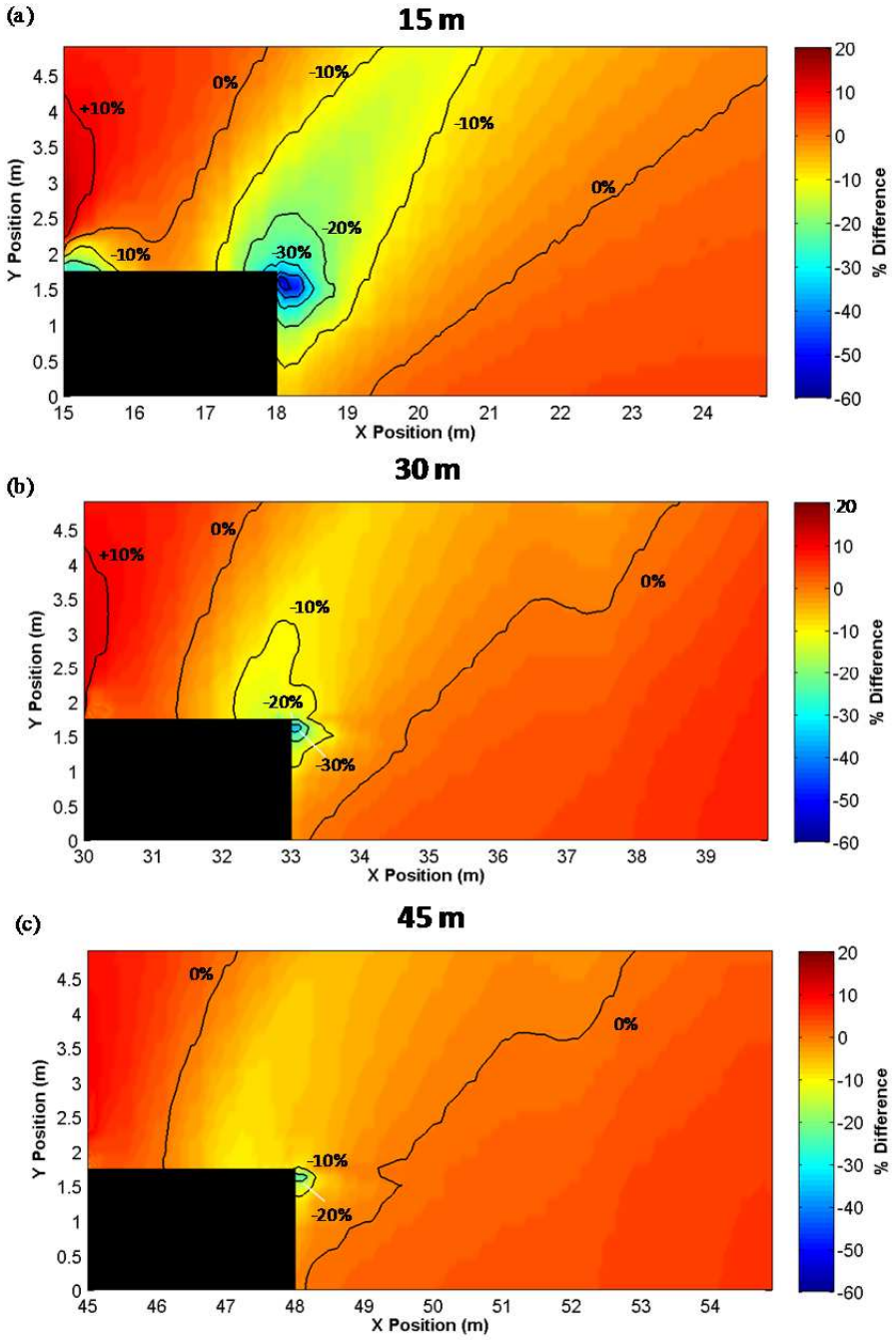

Figure 9: Visualisations showing percentage differences in Is^+ around fixed target obstructions at: (a) 15 m; (b) 30 m and (c) 45 m.

500 kg simulations

Equivalent analyses were performed with a 500 kg TNT_e charge mass to determine the recommended separation distances for 0% interference under these conditions (Table 3).

Table 3: Recommended clear separation distances to achieve 0% interference for a 500 kg charge.

Fixed Target Location \ Variable Target Location	15 m	20 m	25 m	30 m	35 m	40 m	45 m	50 m
15 m	6.28	3.28	5.43	6.91	7.96	8.79	9.44	9.94
20 m		6.26	4.03	6.61	8.43	10.7	11.4	12.01
25 m			6.27	4.71	7.63	9.60	11.0	12.04
30 m				6.97	5.40	8.46	10.5	12.0
35 m					7.54	6.06	9.19	11.3
40 m						8.07	6.57	9.76
45 m							8.62	7.05
50 m								9.02

The angle of the limit of interference for fixed target obstructions at different stand-off ranges in 500 kg simulations has also been presented in Table 4 with percentage differences from 100 kg charge simulations in brackets.

Table 4: Angles of the limit of interference for a 500 kg charge analysis (% difference from Table 1 100 kg charge mass in brackets).

		Angle (°)	
		Ps^+	**Is^+**
Target Stand-off Range	15 m	42.0 (+15.4%)	58.6 (+8.12%)
	20 m	35.0 (+12.5%)	56.3 (+11.3%)
	25 m	30.7 (+9.64%)	54.8 (+11.2%)
	30 m	27.6 (+7.39%)	54.5 (+11.7%)
	35 m	24.9 (+2.47%)	55.5 (+12.1%)
	40 m	22.9 (-1.29%)	57.1 (+11.7%)

The data shows that, similar to the angles given in the 100 kg analysis (Table 1), the angle for the limit of Is^+ interference remains relatively constant between 20 m and 40 m target ranges. Consequently percentage differences between 100 kg and 500 kg charge simulations are also similar. With regards to the angle for the limit of Ps^+ interference, there is a decrease in angle at increasing target stand-off range. Interestingly, the percentage differences between 100 kg and 500 kg charge simulations also decrease with increasing stand-off range to the point where the 500 kg angle is smaller than the 100 kg angle at 40 m.

DISCUSSION

The present study concerned the use of Air3D hydrocode simulations to identify the differences in incident peak overpressure and positive phase impulse with and without a fixed target obstruction present. The simulations were used to identify the separation distances at which different percentage difference interference thresholds were achieved for a 100 kg TNT_e targets between 15 m and 50 m.

The results from the analyses show that, in all cases, a greater separation distance was required to achieve free-field equivalent Is^+ values than Ps^+ values. Consequently, the separation distance required to attain the free-field Is^+ value was adopted in all recommendations.

A recommendation table was generated (Table 2) that provides guidelines for cubicle positioning in 100 kg arena blast trials. Recommended use for these guidelines is that engineers consider a fixed target at a given range and use the tables to identify the required separation for any neighbouring cubicles.

Further simulations were conducted with 500 kg charge masses to evaluate the differences from equivalent 100 kg simulations. The results from the 500 kg simulations show that although, in most cases, an expected greater separation was required they do not follow any conventional scaling approach. Consequently, the results from this study should not be used to infer relationships at greater charge masses.

When the cubicle was positioned at greater stand-off distances from the charge (Figure 8, Figure 9), the interference effects to nearby pressure fields, particularly at the limit of interference, remained relatively constant. Consequently, for practical purposes, the results from the 15 m cubicle simulations could be inferred more widely. This also conveniently introduces a degree of conservatism to account for modelling inaccuracies and experimental variability.

CONCLUSIONS

In large-scale arena blast trials, the positioning of cubicles around a central charge can have a significant effect on the economic cost and experimental accuracy of results. Numerical modelling was used extensively to identify the required separation distances to achieve free-field equivalent Ps^+ and Is^+ values for interference-free positioning of neighbouring targets. The study indicated that, for targets at the same stand-off range, separations of between 3.88 m and 6.92 m were required to achieve free-field equivalency. For targets at different stand-off ranges an angle of at least 54.2° from the front corner of the cubicle has been shown to achieve free-field equivalent conditions. A recommendation table (Table 2) has been generated to provide precise positioning for cubicles at different stand-off ranges.

ACKNOWLEDGEMENTS

The analysis on which this paper is based was conducted as part of an ongoing programme of research and development, funded and directed by the Centre for the Protection of National Infrastructure (CPNI).

REFERENCES

[1] Ballantyne, G. J., Whittaker, A. S., Dargush, G. F. and Aref, A. J. (2009) 'Air-blast effects on structural shapes of finite width', *Journal of Structural Engineering*, 136 (2), pp 152–159.

[2] Remennikov, A.M. and Rose, T.A. (2007) Predicting the effectiveness of blast wall barriers using neural networks. *International Journal of Impact Engineering*, 34 (12), pp.1907-1923.

[3] Rickman, D. D. and Murrell, D. W. (2007) 'Development of an improved methodology for predicting airblast pressure relief on a directly loaded wall', *Journal of Pressure Vessel Technology*, 129 (1), pp 195–204.

[4] Rigby, S., Tyas, A., Bennett, T., Fay, S., Clarke, S. and Warren, J. (2014) 'A numerical investigation of blast loading and clearing on small targets', *International Journal of Protective Structures*, 5 (3), pp 253–274.

[5] Rose, T.A., Smith, P.D. and Mays, G.C. (1995) The effectiveness of walls designed for the protection of structures against airblast from high explosives. *Proceedings of the Institution of Civil Engineers. Structures and Buildings*,110 (1), pp.78-85.

[6] Shi, Y., Hao, H. and Li, Z. X. (2007) 'Numerical simulation of blast wave interaction with structure columns', *Shock Waves*, 17 (1–2), pp 113–133.

[7] Tyas, A., Warren, J. A., Bennett, T. and Fay, S. (2011) 'Prediction of clearing effects in far-field blast loading of finite targets', *Shock Waves*, 21 (2), pp 111–119.